NENE 2015 September 14-17 PORTOROŽ SLOVENIA
24th International Conference Nuclear Energy for New Europe

Temperature Distribution in the Pool of TRIGA Mark II Reactor During Heating Transient

Romain Henry, Marko Matkovič
Jožef Stefan Institute, Reactor engineering division R4
Jamova 39
SI-1000 Ljubljana, Slovenia
romain.henry@ijs.si, marko.matkovič@ijs.si

ABSTRACT

Temperature fields within the pool of the JSI TRIGA MARK II nuclear research reactor were measured to collect data for validation of the thermal hydraulics computational model of the reactor tank. In this context temperature of the coolant was measured simultaneously at sixty different positions within the pool during operation. The obtained data not only revealed local peculiarities of the cooling water dynamics inside the pool but also allowed for better estimation of the coolant bulk velocity within the pool. Natural convection in the pool was simulated with a Computational Fluid Dynamics code. A relatively simple CFD model based on Unsteady RANS turbulence model was found to be sufficient for accurate prediction of the temperature fields in the pool during the reactor operation. Our results show that the simple geometry of the TRIGA pool reactor makes it a suitable candidate for a simple natural circulation benchmark in cylindrical geometry.

1 INTRODUCTION

The TRIGA MARK II research reactor at the Jožef Stefan institute (JSI) is a typical 250 kW TRIGA reactor, which is used for various applications: such as Neutron Activation Analysis (NAA), Neutron Radiography and Tomography, education and training, radiation hardness studies and benchmark experiments for verification and validation of computer codes. It is a light water reactor cooled by demineralised water that flows through the reactor core by natural convection. The core of TRIGA reactor is placed at the bottom of an open tank with 5 m of water column above it. The core has a cylindrical configuration with 91 designed locations to accommodate fuel elements or other components such as control rods, a neutron source and irradiation channels. Elements are arranged in six concentric rings each having 1, 6, 12, 18, 24 and 30 locations, respectively. The experiment and CFD simulations, described in the present work, make the JSI TRIGA reactor one of the most carefully studied nuclear reactors, not only from the neutronic, but also from the thermal hydraulic point of view.

2 EXPERIMENTAL SET UP

Whereas the TRIGA Mark II research reactor at JSI was studied in great detail from neutron physics point of view, very few experiments related to thermal hydraulics were performed. As a result, the number of the available experimental results on velocity and temperature fields in the pool is limited, which makes the validation of the TRIGA thermal-hydraulics model impossible. Therefore, a set of experiments was run to measure the

temperature field of the coolant as accurately as reasonable while taking into account a number of limitations imposed by the nature of the experiments. Limited space available in the tank above the reactor core and the request for reduced generation of radioactive waste have dictated the construction of the supporting structure in aluminium, which, when activated, has a short decay half-time. It was custom built to perfectly fit into the pool with all the obstacles inside it (control rods, irradiation channel, pneumatic system) and to provide rigid support for the temperature sensors. Material of the K-type thermocouples (TCs), made of nickel, chrome and aluminium, was also chosen in order to limit the production of waste while keeping the accuracy of the sensor sufficiently high. Safe operation of the reactor had not to be compromised and specific measures had to be taken to reduce activation of the introduced material to the minimum. Therefore, experimental procedure was prepared in agreement with the requirement imposed by the safety committee of the reactor [1].

3 CFD MODEL

The CFD simulations were performed with the commercial code ANSYS® CFX [2]. The geometry of the pool, a 6.5 m high cylinder of diameter 2 m, was reproduced. Core was modelled with 61 fuel rods, 4 control rods and 5 irradiation channels of similar geometry (Figure 1). All these solid or air filled volumes were cut out from the computational domain.

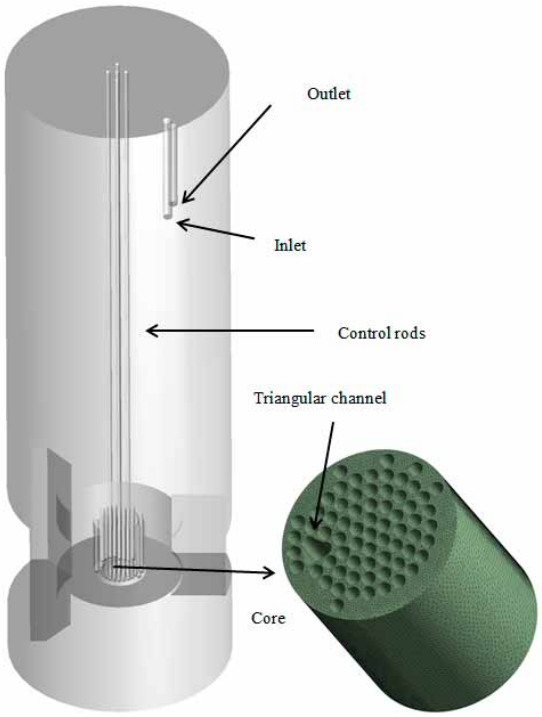

Figure 1: Geometrical model of TRIGA with control rods fully modelled (left). Mesh details in the core region (right).

In the same way the volumes occupied by the graphite reflector and two thermal columns were also cut out from the computational domain. Other structures taken into account were 4 control rod guides that span from the core towards the surface of the pool. These metal guide rods represent a non-negligible flow resistance in the region of the pool with the largest fluid velocities. Other structures in the pool were found to represent a minor flow resistance to the natural convection as they lay within the regions where the natural circulation velocities are at least ten times lower than in the region above the core. Inlet and

outlet pipes in the upper section of the pool were also modelled, although their pipes do not represent a significant obstruction for the flow.

Basic equations for natural circulation of incompressible fluid are described in [3]. The domain is filled by demineralised water with constant material properties. Buoyancy is modelled through Boussinesq approximation, turbulence is modelled with k-ε RANS model. Heat produced within the fuel is taken into account as a specified heat flux boundary conditions. Constant heat flux was assumed for each fuel rod in the radial direction and the axial distribution had the same chopped cosine shape for all fuel rods. Other thermal boundary conditions were adiabatic walls, except for a single run where wall heat losses were assumed at the walls of the pool. The domain was then discretized; different meshes were considered to ensure that our solutions were grid independent. The grid contains 12 million volumes with a typical dimension length varying from 8 mm to 5 cm. Non-structured grid of tetra elements was used - more suitable for complex geometries of the core and structures above the core. Convergence of the numerical solutions was achieved within 0.5 % imbalance criteria. The temperature of sixty points corresponding, within position errors, to the sixty TCs were monitored and used for verification of the simulations.

Experimental and simulated results of heating of the reactor are presented in this paper, although some other modes of operation were also measured and analysed. CFD temperature field is presented for various points corresponding to the positions of the TCs (Figure 2).

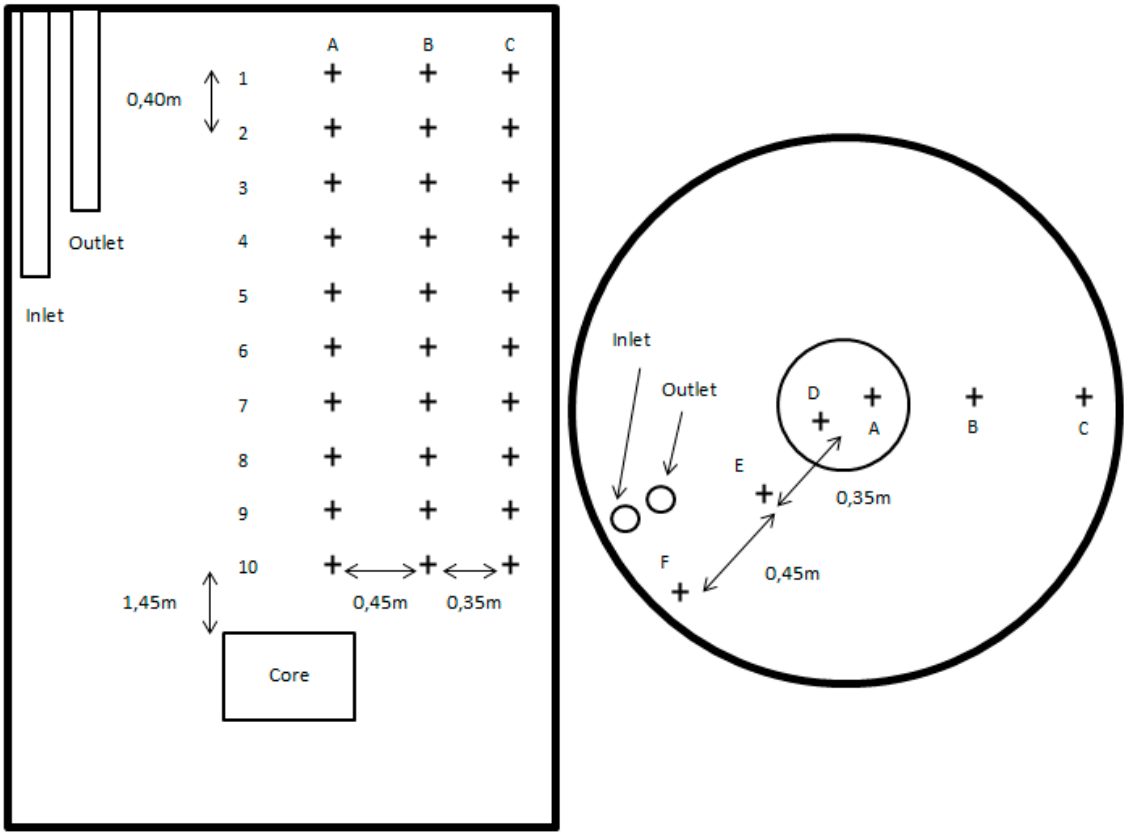

Figure 2: Schematic of the side and top view of the TRIGA reactor pool with the positions of the thermocouples. Letters define columns and numbers define rows in the grid. The grid (D, E, and F) is inserted 10 cm deeper than the grid (A, B, C)

4 RESULTS

The first transient considered was to run the reactor at full power (250 kW) for 70 minutes without external cooling. This makes this case a pure natural convection case with a Rayleigh number value of around 10^{13}. The initial conditions referred to a cold reactor at average water temperature slightly above 18 °C. The energy released by the core heated up the fluid and induced natural convection. Temperatures in the pool were being recorded during the entire period of the pool heating, which made the detailed interpretation of the whole transient possible. Furthermore, transient simulation of the pool model was performed and the temperature field of the coolant was calculated for the entire pool. Figure 3 shows the course of the measured and calculated coolant temperature at various positions (Figure 2) in the pool. It was observed that temperature distribution along the columns B and E as well as C and F have very similar profile. While the basic flow pattern within the tank was intuitively foreseen, several peculiarities were noted during the experiment and simulations.

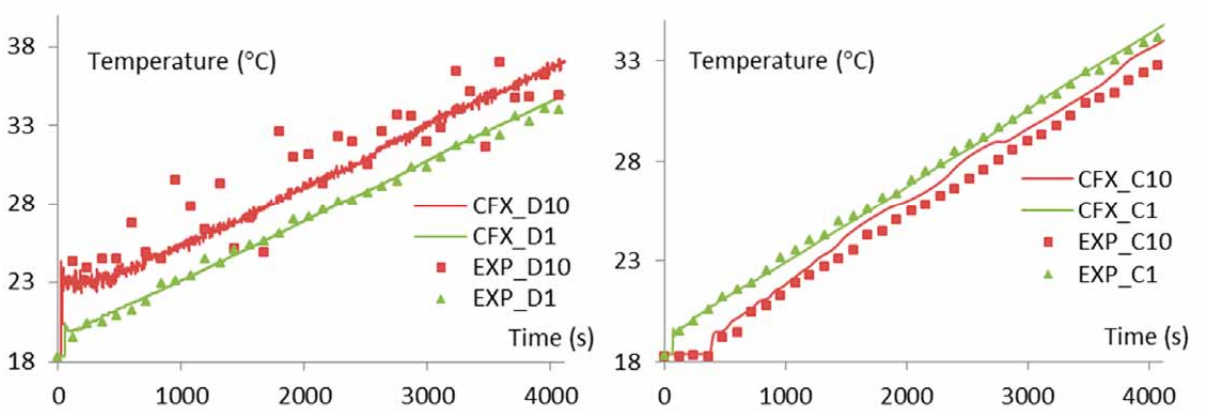

Figure 3: Coolant temperature at various positions in the pool during the heating-up process. Symbols - measurement, solid lines - simulations.

It can be observed that measured temperature variation above the core increases with depth, while the variation is notably less pronounced at the top of the pool. This can be explained by different temperatures at the exit of the channels between the various fuel rods shown in Figure 4 (simulation).

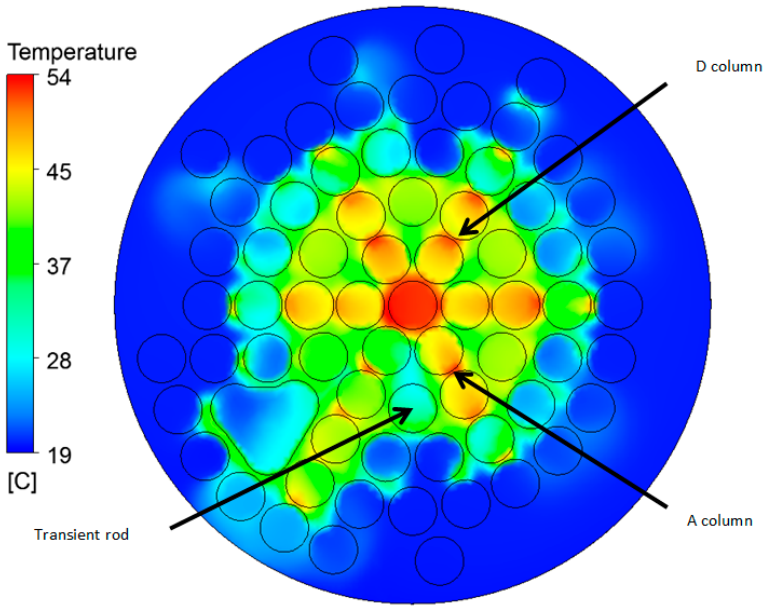

Figure 4: Calculated temperature distribution just above the core at t = 1000 s.

Measured temperature fluctuations are not predicted with the CFD model using RANS turbulent model since CFX is solving equation for average quantities. Nevertheless, reproduction of the course of coolant temperature is achieved. While it was observed that column B, C, E and F have very similar profile, some differences were found between A and D column. Figure 4 presents the calculated temperature profile just above the top of the fuel. From this picture it appears that only the area limited to the radius of the active core encounters the chaotic behaviour induced by the mixing arising directly from the core with the cold water of the pool. It was foreseen that temperature at position A10 was over-predicted compared to the one at position D10. One explanation is the proximity of the zero-power transient rod. Since this rod is not having any fuel part it creates a larger temperature gradient in its neighbourhood making the flow more chaotic. Furthermore one can see that temperature difference just above the core can be up to 30 °C explaining the temperature oscillation in position D10 observed especially in the experimental and in the lesser extent also in numerical results.

Figure 5 shows that a steady state natural convection with increasing mean pool temperature is established after about 500 seconds. Mean pool temperature is slowly rising all the time, while the relative temperature differences remain unchanged. It means that after about 500 seconds one needs only one or two TCs in the pool to estimate the average pool temperature.

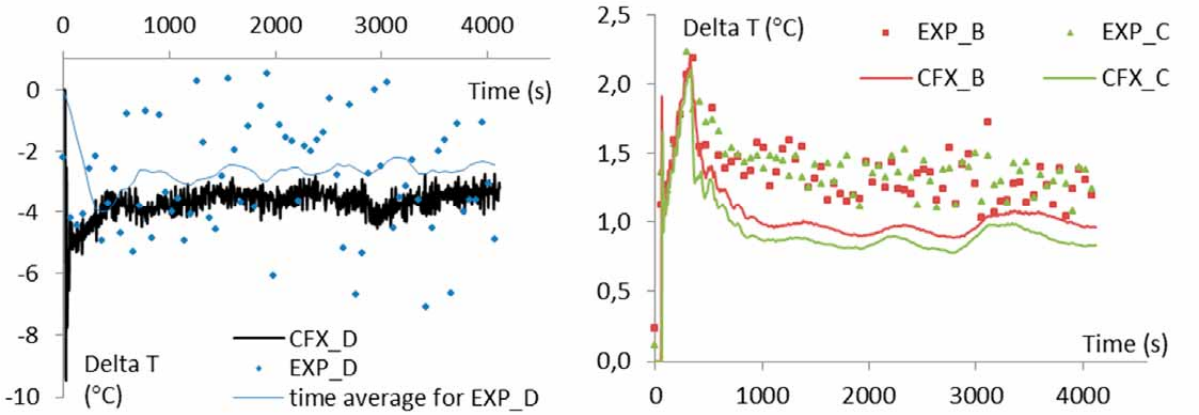

Figure 5: Temperature difference between top (position 10) and bottom (position 1) for three thermocouple columns.

From this observation, the transient can be split into two parts: the first 500 seconds is the time needed for the development of the steady natural circulation flow. In the remaining part, velocity field remains steady, while nearly linear trend is observed for temperatures in all points across the reactor pool.

During the first 500 seconds the heat released into the water initiates the motion of the flow. Correlating temperature perturbation of the neighbouring TCs provided an indication of the propagation fluid velocity within the reactor tank during the onset of the natural convection. Deduced propagation velocities between the uppermost and lowest positions are shown in the table 1. Relative uncertainties were estimated to a few percent. One explanation could be the decision to model the start-up of the reactor as a step function in CFX, while during operation 20 seconds were needed for the transition from 20 % to 100 % of the full power. From this observation, the time zero was the time when the reactor reached half of its total power.

It can be seen that the detection time of the temperature perturbation induced by the start of the reactor is rather well reproduced for every point.

Table 1: Position and time delay of measured and calculated temperature perturbations; estimation of the vertical component of the propagation velocity. Time zero corresponds to the start of the reactor.

Thermocouple position	Detection time (s) experimental value	Detection time (s) calculated value	v_z (cm/s) from experimental value	v_z (cm/s) from calculated value
A1	57	54		
A10	6	14	7,1	9
C1	65	62		
C10	359	352	-1,2	-1,2

Further insight into the transient leading into the steady velocity field is shown in figure 6, where vertical components of the local velocities are given in the points that correspond to the positions of the TCs. Unlike the velocities in table 1, which are evaluated during the development of the natural convection, the Figure 6 represents local velocities, which were not measured, but are obtained from the simulations. The velocities at position A10 show oscillations around a mean value of 18 cm/s. Other positions exhibit perturbations related to the onset of the natural convection and steady state behaviour after approximately 300 seconds.

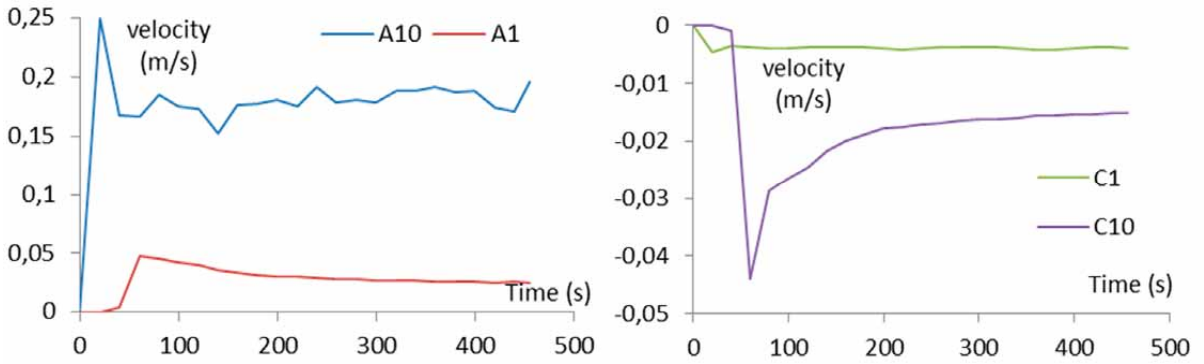

Figure 6: Calculated coolant vertical velocities at various positions in the pool during the heating-up

From the measurements of the initial temperature perturbations, a schematic reconstruction of the induced secondary flow during the reactor heating can be obtained: the propagation velocities are presented in figure 7. Notably higher velocity of the rising water induces the secondary flow of the coolant, directed from the side toward the centreline of the pool. There, the two masses are intensively mixed. As a result, during the heating, a significant difference between the temperature profiles in the centre of the pool is observed with respect to the dynamics at the edge of the tank.

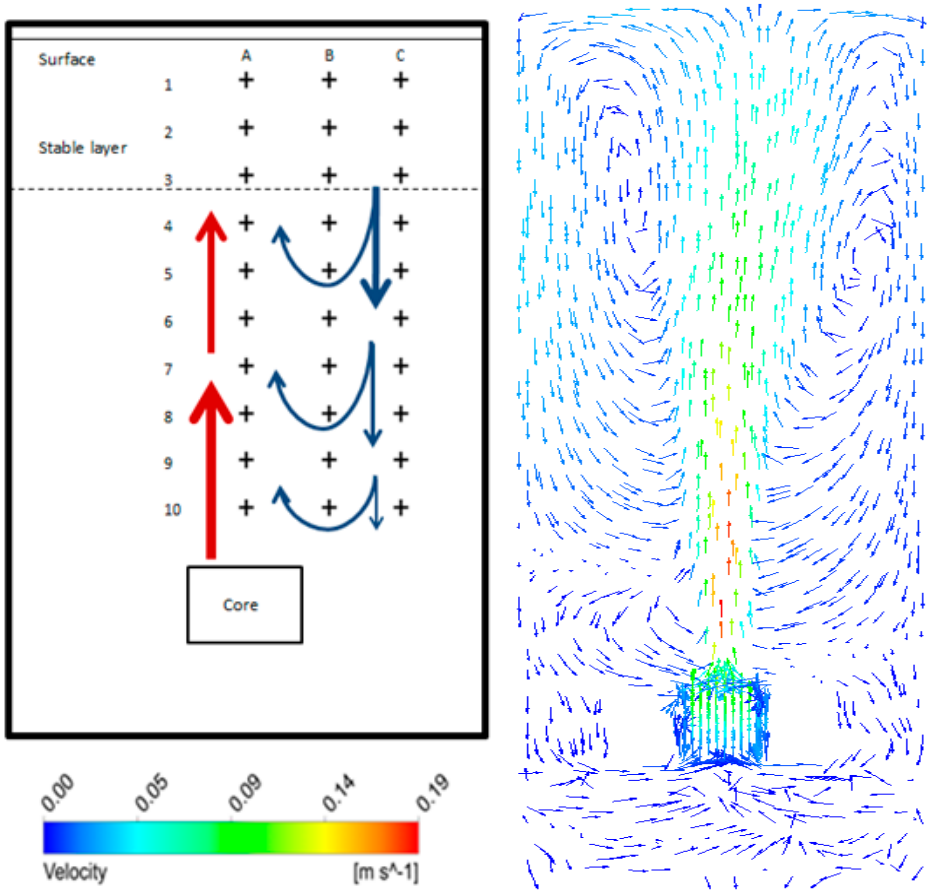

Figure 7: Scheme of the natural convection and the induced secondary flow during the heating-up (left) and the predicted velocity field by the simulation in the plane XZ (right)

In fact, the columns of the TCs that are closer to the wall (B, C, E and F) reflect almost the same vertical temperature profiles (figure 8), whereas the established temperatures along the centreline in the pool exhibit the opposite trend. The amplitude of the temperature variations within the pool remains almost constant in time, which implies a remarkably stable column of the rising fluid. Variation of the position of the two structures has revealed that the intensive mixing takes place in a rather narrow column above the centre of the core. There, the highest temperature oscillations were measured above the core and the lowest values were recorded just below the surface of the pool. The simulation has shown that the least affected region in the pool without active cooling was found to be the bottom annulus below the core.

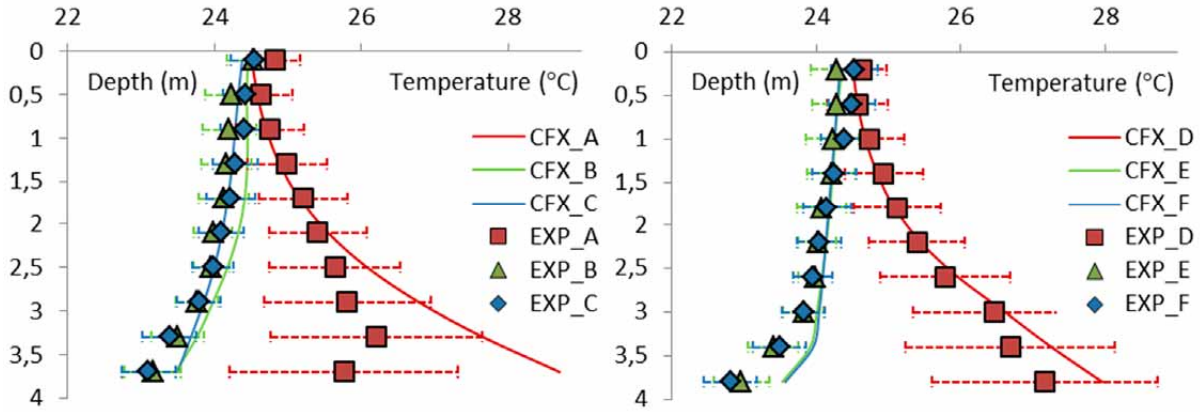

Figure 8: Measured and calculated temperature axial profile during heating up

As the vertical velocity of the water, sinking around the perimeter of the pool towards the bottom, is gradually reduced due to the secondary flow, the water mass there is delivered with considerable delay, which leads to the lowest measured temperatures in the tank. Lower temperature differences were observed further away from the core up to the point where no significant difference was measured in the uppermost layer of the pool. However, once the steady velocity field was established the average temperature started increasing linearly at the same rate.

5 CONCLUSION

A CFD model of the reactor pool was built. Analysis of the reactor operation without external cooling system reveals that a transition period, around 500 seconds, was needed for the natural convection profile to develop. During this phase, the propagation of the temperature perturbation, induced by the start-up of the reactor, was recorded by measuring time-lags at which the perturbation was detected by the different thermocouples. Furthermore, an estimation of the propagation velocities was made. Predicted velocity fields were in good agreement with all the prior experimental results. When the velocity field of the flow became steady, the temperature of the pool started increasing quasi linearly. It was observed that most of the mixing was taking place within the narrow plume of the rising fluid directly above the core. Two possible reasons were identified. One is associated to the uneven temperature distribution of the coolant rising from the reactor core while the other is associated to the secondary flow of the cold sinking coolant from the side of the pool. On the other hand, no significant temperature fluctuations were observed outside the narrow column where temperatures were rising almost linearly with time. Those observations were precisely reproduced by the model.

ACKNOWLEDGMENTS

The authors gratefully acknowledge the valuable contributions of the reactor operator staff at JSI, in particular from Anže Jazbec, Darko Kavšek, Sebastjan Rupnik and Marko Rosman, for their help from the conception to the realization of the experimental campaign and of the Research group P2-0026.

REFERENCES

[1] R. Henry, M. Matkovič, I. Tiselj, "Temperature distribution measurements in the pool of TRIGA mark II reactor", 5th International Youth Conference on Energy 2015, 27th May - 30th May 2015, Pisa, Italy.

[2] ANSYS Inc., User's guide, ANSYS 14.0 Documentation, 2011

[3] L.D. Landau, E.M. Lifshitz, Fluid Mechanics (Volume 6 of A Course of Theoretical Physics) Pergamon Press 1959.